Molecular determinants of the physicochemical properties of a critical prion protein region comprising residues 106–126

Mario SALMONA*[1], Paolo MALESANI*, Luca DE GIOIA†, Stefano GORLA*, Maurizio BRUSCHI*, Antonio MOLINARI‡, Franco DELLA VEDOVA‡, Barbara PEDROTTI§, Maria Anna MARRARI§, Tazeen AWAN§, Orso BUGIANI§, Gianluigi FORLONI* and Fabrizio TAGLIAVINI§

*Istituto di Ricerche Farmacologiche 'Mario Negri', Via Eritrea 62, 20157 Milano, Italy, †Dipartimento di Chimica Inorganica, Metallorganica e Analitica, Università degli Studi di Milano, Via Venezian 21, 20133 Milano, Italy, ‡Pharmacia and Upjohn, Via Giovanni XXIII, 20014 Nerviano, Milano, Italy, and §Istituto Nazionale Neurologico 'Carlo Besta', Via Celoria 11, 20133 Milano, Italy

Prion diseases are marked by the cerebral accumulation of conformationally modified forms of the cellular prion protein (PrP^C), known as PrP^{res}. The region comprising the residues 106–126 of human PrP seems to have a key role in this conformational conversion, because a synthetic peptide homologous with this sequence (PrP106–126) adopts different secondary structures in different environments. To investigate the molecular determinants of the physicochemical characteristics of PrP106–126, we synthesized a series of analogues including PrP106–126 H_D, PrP106–126 A and PrP106–126 K, with L-His → D-His, His → Ala and His → Lys substitutions respectively at position 111, PrP106–126 NH_2 with amidation of the C-terminus, PrP106–126 V with an Ala → Val substition at position 117, and PrP106–126 VNH_2 with an Ala → Val substitution at position 117 and amidation of the C-terminus. The analysis of the secondary structure and aggregation properties of PrP106–126 and its analogues showed the following. (1) His^{111} is central to the conformational changes of PrP peptides. (2) Amidation of the C-terminal Gly^{126} yields a predominantly random coil structure, abolishes the molecular polymorphism and decreases the propensity of PrP106–126 to generate amyloid fibrils. (3) PrP106–126 V, carrying an Ala → Val substitution at position 117, does not demonstrate a fibrillogenic ability superior to that of PrP106–126. However, the presence of Val at position 117 increases the aggregation properties of the amidated peptide. (4) Amyloid fibrils are not required for neurotoxicity because the effects of PrP106–126 NH_2 on primary neuronal cultures were similar to those of the wild-type sequence. Conversely, astroglial proliferation is related to the presence of amyloid fibrils, suggesting that astrogliosis in prion encephalopathies without amyloid deposits is a mediated effect rather than a direct effect of disease-specific PrP isoforms.

Key words: amyloid, prion protein peptides, secondary structure modifications.

INTRODUCTION

Prion diseases such as scrapie of sheep and goats, bovine spongiform encephalopathy, and Creuzfeldt–Jakob disease ('CJD') and Gerstmann–Sträussler–Scheinker disease (GSS) of humans are characterized by the accumulation of abnormal forms of the cellular prion protein (PrP^C), termed PrP^{res}, in the brain [1]. In contrast with PrP^C, PrP^{res} is partly resistant to digestion with protease and has a marked tendency to form insoluble aggregates and amyloid fibrils [2–4]. The accumulation of PrP^{res} and PrP amyloid in the brain is thought to be responsible for the nerve cell degeneration, astrogliosis and activation of microglial cells observed in prion-related encephalopathies [5–7].

NMR studies of recombinant murine PrP indicate that the normal protein is composed of two structurally distinct moieties: an extended N-terminal segment (residues 23–125) with features of a flexibly disordered polypeptide chain, and a well-defined globular domain (residues 126–231) with three α-helices and a two-stranded anti-parallel β-sheet [8–10]. The transition from PrP^C to PrP^{res} involves a striking conformational change with a decrease in α-helical secondary structure (from 42 % to 30 %) and a remarkable increase in β-sheet content (from 3 % to 43 %) [11,12]. This rearrangement is accompanied by the acquisition of abnormal physicochemical properties, including insolubility in non-denaturing detergents and partial resistance to digestion with proteinase K.

Previous studies have shown that a synthetic peptide homologous with residues 106–126 of human PrP (PrP106–126) exhibits some of the pathogenic and physicochemical properties of PrP^{res} [5–7,13–15]. Like PrP^{res}, this peptide causes nerve cell death by apoptosis and induces hypertrophy and proliferation of astrocytes and activation of microglial cells *in vitro* [5–7]. It is noteworthy that the neurotoxicity of the peptide requires the expression of endogenous PrP, which is consistent with the observation that neuronal death in scrapie infection *in vivo* is dependent on PrP^C synthesis [16,17]. It also increases the membrane microviscosity of a variety of cells, including neurons and astrocytes [18,19]. PrP106–126 shows a remarkable conformational polymorphism, acquiring different secondary structures in different environments [15]; nevertheless, it tends to adopt a β-sheet conformation in buffered solutions and aggregates into amyloid fibrils that are partly resistant to digestion with protease. These data indicate that the PrP region including residues 106–126 might be the nido at which conformational change is initiated in the conversion of PrP^C to PrP^{res}. This view is supported by the observation that the N-terminal half of PrP

Abbreviations used: GSS, Gerstmann–Sträussler–Scheinker; PrP, prion protein; PrP^C, cellular PrP; PrP^{res}, pathological and protease-resistant isoform of PrP; PrP106–126, synthetic peptide comprising residues 106–126 of human PrP; PrP106–126 H_D, with L-His → D-His substitution at position 111; PrP106–126 A, with His → Ala substitution at position 111; PrP106–126 K, with His → Lys substitution at position 111; PrP106–126 V, with Ala → Val substitution at position 117; PrP106–126 NH_2, with amidation at the C-terminus; PrP106–126 VNH_2, with Ala → Val substitution at position 117 and amidation of the C-terminus; TFE, 2,2,2-trifluoroethanol.

[1] To whom correspondence should be addressed (e-mail salmona@irfmn.mnegri.it).

(residues 23–125) is highly flexible and more susceptible to structural transitions than the C-terminal globular domain, and that the deletion of residues 23–88 does not prevent the conversion of PrP^{C} to PrP^{res}, whereas the ablation of residues 108–121 or 122–140 together with residues 23–88 does so [20].

The present study was undertaken to investigate the molecular determinants of the conformational polymorphism of PrP106–126 and its propensity to form amyloid fibrils. Several peptide analogues containing amino acid changes were synthesized and their physicochemical properties were compared with the those of wild-type sequence. The selection of amino acid changes was based on the assumption that the conformational polymorphism and fibrillogenic properties of PrP106–126 depend at least in part on the presence of an ionizable residue (i.e. His^{111}) between the hydrophilic and hydrophobic domains of the peptide, and on electrostatic and hydrophobic interactions between molecules conferring stability to the β-sheet configuration. We also analysed the effects of the Ala → Val substitution at position 117, a mutation linked to GSS disease. This effect was evaluated on the wild-type protein and the C-terminal amidated form of PrP106–126 (PrP106–126 NH_2). The latter was used because the amidation of the C-terminus greatly decreases the fibrillogenic properties of the peptide and allows the more effective detection of the influence of the amino acid substitution. Finally, we investigated how the physicochemical changes resulting from the amidation of the C-terminus and the Ala → Val substitution at residue 117 affected the biological activity of the peptide.

EXPERIMENTAL

Peptide synthesis

The following peptides were used for the study: PrP106–126 (K^{106}TNMKHMAGAAAAGAVVGGLG; single-letter codes); PrP106–126 H_D, with an L-His → D-His substitution at position 111; PrP106–126 A (K^{106}TNMK<u>A</u>MAGAAAAGAVVGGLG), with an His → Ala substitution at position 111; PrP106–126 K (K^{106}TNMK<u>K</u>MAGAAAAGAVVGGLG), with a His → Lys substitution at position 111; PrP106–126 V (K^{106}TNMKHMAGAA<u>V</u>AGAVVGGLG), with an Ala → Val substitution at position 117; PrP106–126 NH_2 (K^{106}TNMKHMAGAAAAGAVVGGL<u>G-NH$_2$</u>), with amidation at the C-terminus; and PrP106–126 VNH_2 (K^{106}TNMKHMAGAA<u>V</u>AGAVVGGL<u>G-NH$_2$</u>), with an Ala → Val substitution at position 117 and amidation at the C-terminus. The peptides were synthesized by solid-phase chemistry and purified by reverse-phase HPLC, as described previously [15]. Purity was always greater than 95%.

Preparation of peptide solutions

Peptides were dissolved in deionized water at 0.75 or 1.5 mg/ml (stock solutions). Under these conditions they were soluble, as deduced by the absence of a visible pellet after centrifugation at 13000 ***g*** for 10 min. The stock solutions were stable for 2 weeks at −80 °C, as determined by reverse-phase HPLC (see below). Aliquots of stock solutions were added to 200 mM phosphate buffer, pH 5.0 or 7.0, to obtain final peptide concentrations of 0.25, 0.50, 0.75 or 1.0 mg/ml phosphate buffer. The actual concentration of each peptide in phosphate buffer was determined by HPLC analysis immediately after preparation of the samples and was used as the zero-time value in sedimentation experiments. To investigate how the α-helix-stabilizing solvent 2,2,2-trifluoroethanol (TFE) influenced the secondary structure, the peptides were first suspended in phosphate buffer, pH 5.0, at a concentration of 0.5 mg/ml; TFE was then added to the samples to a final concentration of 50% (v/v).

CD spectroscopy

The analysis was performed on 0.25 mg/ml peptide suspensions in phosphate buffer, pH 5.0 and 7.0, or phosphate buffer containing TFE, prepared as described above. The spectra were recorded after incubation for 1 h in quartz cells, with an optical path of 0.1 cm, by using a Jasco J-500 dichograph (Tokyo, Japan) at a scan speed of 2 nm/min. Mean residue ellipticities were calculated by using the following equation: $(\theta)_M = 3300AM/Cl$, where A is the observed dichroic absorbance, l is the path length in cm, C is the concentration of the peptide in g/l and M is the mean residue weight. The percentages of the secondary structure of the peptides were calculated by the method of Yang et al. [21].

Turbidity measurements

The analysis was performed on 0.25 mg/ml peptide suspensions in phosphate buffer, pH 5.0 and 7.0. The turbidity of the samples was determined immediately after their preparation (zero time) and after incubation for 24 h at room temperature, with a Perkin–Elmer Lambda 10 spectrophotometer at 600 nm.

Sedimentation experiments

The study was performed on 0.75 mg/ml peptide suspensions in phosphate buffer, pH 5.0. Aliquots of 20 μl were incubated at 37 °C for 0, 1, 2, 4 and 24 h, then chilled on ice and centrifuged at 13000 ***g*** for 10 min at 4 °C. Supernatant (2 μl) was injected into an HPLC apparatus equipped with a 3.9 mm × 150 mm Delta-Pak C_{18} column, a model P 4000 pump, a UV 2000 variable-wavelength detector, an AS 3000 autosampler (Waters, Milford, MA, U.S.A.) and an SP 4400 integrator operated in both peak height and area modes (Thermo Separations Products, Riviera Beach, FL, U.S.A.). MilliQ water/acetonitrile (75:25, v/v) containing 0.1% (v/v) trifluoroacetic acid was used as eluent, at a flow rate of 1 ml/min. The column eluates were monitored at 214 nm. The peptide concentrations in the supernatant at different times were expressed as percentages of the corresponding values determined at zero time.

Light and electron microscopy

Peptides were suspended in phosphate buffer, pH 5.0, at a final concentration of 1 mg/ml. After incubation for 24 h at 20 °C, 50 μl of each suspension was air-dried on gelatin-coated slides, stained with 1% (w/v) aqueous thioflavin S and analysed by fluorescence microscopy. For electron microscopy, 5 μl of suspension was applied to Formvar-coated nickel grids, negatively stained with 5% (w/v) uranyl acetate and observed in an electron microscope (EM 109, Zeiss, Germany) at 80 kV.

Nerve cell cultures

Cerebral cortex was dissected from fetal rat brains on embryonic day 17. Cortical cells were dissociated and plated in 24-well dishes (3.5×10^5 cells per dish) at 37 °C in humidified air/CO_2 (19:1), as described previously [5]; 24 h after being plated, the cultures were exposed to PrP106–126, PrP106–126 NH_2 or

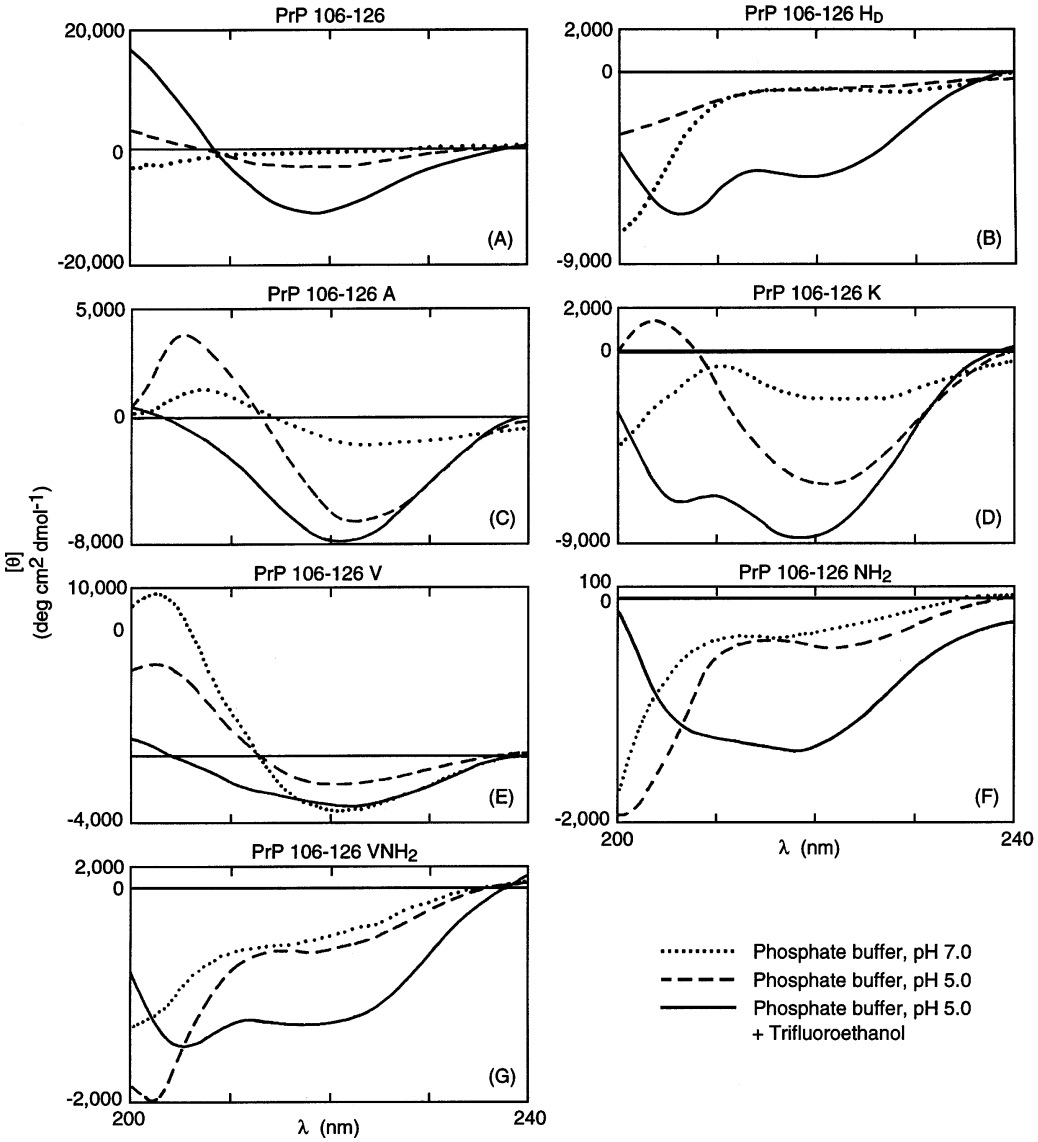

Figure 1 CD spectra of PrP106–126 and its analogues

PrP106–126 VNH_2 at 50 μM for 7 days. Control cultures were exposed to vehicle only. Cell viability was then assessed by staining with Crystal Violet [0.5% in water/methanol (4:1)]. After washing, cells were dried and the staining intensity was determined densitometrically with an image analyser (IBAS 2.0; Zeiss, Cologne, Germany) [22].

Astroglial cultures

Glial cell cultures were prepared from newborn rat pups as described [6]. After 10 days of culture, flasks containing mixed glial cells were given fresh medium and shaken at 37 °C for 12–16 h. The supernatant containing microglia and oligodendrocytes was removed and replaced with fresh Dulbecco's modified Eagle's medium. The adherent cells (astrocytes) were then exposed for 5 min to 0.25% trypsin. After the addition of an equal volume of Dulbecco's modified Eagle's medium/10% (v/v) fetal calf serum, the cell suspension was centrifuged and the pellet was resuspended in medium containing 10% fetal calf serum. Cells were plated at a density of 5×10^4 cells/ml [20] and exposed to PrP106–126, PrP106–126 NH_2 or PrP106–126 VNH_2 at 50 μM for 7 days. Control cultures were exposed to vehicle only. Glial proliferation was assessed by staining with Crystal Violet and densitometric analysis [23,24].

RESULTS

Secondary structure of PrP peptides as deduced by CD spectroscopy

In a previous study we showed that PrP106–126 can adopt different conformations in different environments, e.g. a random coil structure in deionized water, a combination of random coil and β-sheet in 200 mM phosphate buffer, pH 7.0, a β-sheet conformation in phosphate buffer, pH 5.0, and an α-helical structure in TFE. A remarkable finding was the stability of the β-sheet secondary structure, which was not affected by the addition of TFE to a solution of the peptide in phosphate buffer, pH 5.0 [15].

Table 1 Percentages of secondary structure in peptide PrP106-126 and its analogues

Results are means ± S.E.M. for at least three different experiments.

Row	Peptide	pH	TFE	Secondary structure (%)			
				α-Helix	β-Sheet	β-Turn	Random coil
A	PrP106–126	5.0	–	22 ± 3	61 ± 4	–	17 ± 4
B		7.0	–	17 ± 2	40 ± 5	4 ± 1	39 ± 2
C		5.0	+	28 ± 5	58 ± 3	2 ± 1	12 ± 5
D	PrP106–126 H_D	5.0	–	5 ± 1	12 ± 5	5 ± 3	78 ± 7
E		7.0	–	4 ± 2	4 ± 3	11 ± 5	81 ± 9
F		5.0	+	48 ± 6	16 ± 3	5 ± 2	31 ± 7
G	PrP106–126 A	5.0	–	15 ± 4	53 ± 6	14 ± 2	18 ± 5
H		7.0	–	13 ± 3	51 ± 5	16 ± 2	20 ± 5
I		5.0	+	25 ± 8	50 ± 10	9 ± 1	16 ± 5
J	PrP106–126 K	5.0	–	22 ± 3	51 ± 6	12 ± 3	15 ± 2
K		7.0	–	9 ± 2	24 ± 5	18 ± 2	51 ± 7
L		5.0	+	40 ± 8	42 ± 10	2 ± 1	16 ± 5
M	PrP106–126 V	5.0	–	25 ± 3	58 ± 8	2 ± 1	20 ± 2
N		7.0	–	14 ± 2	44 ± 5	4 ± 2	38 ± 1
O		5.0	+	22 ± 5	59 ± 9	1 ± 0	18 ± 2
P	PrP106–126 NH_2	5.0	–	5 ± 2	11 ± 5	11 ± 7	73 ± 13
Q		7.0	–	4 ± 3	8 ± 4	12 ± 4	76 ± 11
R		5.0	+	51 ± 7	25 ± 5	5 ± 2	19 ± 7
S	PrP106–126 VNH_2	5.0	–	5 ± 2	15 ± 2	9 ± 5	71 ± 10
T		7.0	–	5 ± 1	19 ± 4	9 ± 2	67 ± 7
U		5.0	+	42 ± 8	22 ± 3	6 ± 3	30 ± 6

To unravel the molecular determinants of these structural properties, we generated PrP106–126 analogues with modifications of single amino acids (substitution of D-His, Ala or Lys for L-His[111]; substitution of Val for Ala[117]; amidation of the C-terminus with or without the substitution of Val for Ala[117]) and analysed the effects of these changes on the conformational polymorphism of the peptides and the stability of the β-sheet conformation. Figure 1 and Table 1 show the CD spectra and percentages of secondary structure of PrP106–126 analogues in phosphate buffer, pH 5.0 and 7.0, and in phosphate buffer, pH 5.0, after the addition of TFE.

The characteristics of PrP106–126 were substantially altered by modifications of His[111]. PrP106–126 H_D showed a striking decrease in β-sheet and α-helical content, with a parallel increase in random coil structure; this effect was observed at both pH 5.0 and 7.0 (Figure 1B, and Table 1, rows D and E). The addition of TFE to PrP106–126 H_D solutions in phosphate buffer markedly enhanced the α-helical content (Figure 1B, and Table 1, row F). PrP106–126 A showed a high proportion of β-sheet secondary structure at both pH 5.0 and 7.0, as indicated by a positive peak with a maximum at 206 nm and a broad negative band centred on 220 nm (Figure 1C, and Table 1, rows G and H); the only difference between the spectra recorded at neutral and acidic pH was the signal intensity, which was much stronger at pH 5.0. The addition of TFE to PrP106–126 A in phosphate buffer resulted in a slight increase in α-helix (Figure 1C, and Table 1, row I). PrP106–126 K adopted a predominantly β-sheet conformation in phosphate buffer at pH 5.0 (Figure 1D, and Table 1, row J); the β-sheet content decreased at pH 7.0 and the random coil became the prevalent secondary structure (Figure 1D, and Table 1, row K). The addition of TFE to PrP106–126 K in phosphate buffer caused an ordered arrangement with equal contributions of α-helix, as deduced by two negative bands at 206 and 220 nm, and β-sheet, as indicated by a more intense, broad negative absorption at 220 nm (Figure 1D, and Table 1, row L).

Table 2 Turbidity measurements on PrP106-126 and its analogues

Peptides were suspended in 200 mM phosphate buffer, pH 5.0 or 7.0, at a concentration of 0.25 mg/ml; and the difference in D_{600} between zero time and after incubation for 24 h at room temperature was calculated. Results are means ± S.E.M. for at least four determinations. *$P < 0.05$ compared with the peptide suspension at pH 5.0 (Student's t test).

Peptide	pH ...	ΔD_{600} between 0 and 24 h of incubation	
		5.0	7.0
PrP106–126		0.085 ± 0.008	0.114 ± 0.032*
PrP106–126 H_D		0.071 ± 0.010	0.078 ± 0.014
PrP106–126 A		0.121 ± 0.005	0.126 ± 0.002
PrP106–126 K		0.075 ± 0.010	0.080 ± 0.011
PrP106–126 V		0.081 ± 0.001	0.110 ± 0.001*
PrP106–126 NH_2		0.064 ± 0.003	0.066 ± 0.003
PrP106–126 VNH_2		0.069 ± 0.002	0.096 ± 0.011*

The substitution of Val for Ala[117] (PrP106–126 V) had no significant effect on the spectral features and structural stability of PrP106–126, which had a high β-sheet content in phosphate buffer (Figure 1E, and Table 1, rows M and N) and also in the presence of TFE (Figure 1E, and Table 1, row O). Amidation of the C-terminal Gly[126] (PrP106–126 NH_2) decreased the propensity to adopt the β-sheet structure in phosphate buffer, at both pH 5.0 and 7.0; under these conditions, the peptide showed a random coil arrangement, as indicated by the strong negative band at 200 nm (Figure 1F, and Table 1, rows P and Q). The addition of TFE to PrP106–126 NH_2 in phosphate buffer, pH 5.0, caused a striking increase in α-helical structure (Figure 1F, and Table 1, row R). The substitution of Val for Ala[117] of the amidated peptide (PrP106–126 VNH_2) slightly changed the spectral features in phosphate buffer, at both pH 5.0 and 7.0; this change consisted of an increased intensity of the negative band at 220 nm, indicating a higher degree of β-sheet secondary structure (Figure 1G, and Table 1, rows S and T). The addition of TFE to PrP106–126 VNH_2 in phosphate buffer, pH 5.0, resulted in an increased α-helical content (Figure 1G, and Table 1, row U); this increase was less pronounced than that observed for PrP106–126 NH_2.

Aggregation properties of PrP106–126 peptides

The ability of PrP106–126 analogues to form macroaggregates was first assessed by turbidity measurements. The peptides were suspended in phosphate buffer, pH 5.0 or 7.0, at 0.25 mg/ml, and the difference in absorbance between zero time and after incubation for 24 h at room temperature was calculated (Table 2). At zero time, no significant differences in optical density were observed between the different peptide suspensions at both pH 5.0 and 7.0; in a typical experiment at pH 5.0, the following initial values (means ± S.E.M. for four replicates) were recorded: PrP106–126, 0.058 ± 0.005; PrP106–126 H_D, 0.055 ± 0.004; PrP106–126 A, 0.065 ± 0.008; PrP106–126 K, 0.055 ± 0.09; PrP106–126 V, 0.062 ± 0.004; PrP106–126 NH_2, 0.051 ± 0.008; PrP106–126 VNH_2, 0.053 ± 0.009. After incubation for 24 h, PrP106–126 suspensions showed an increase in turbidity values that was higher at pH 7.0 than at pH 5.0. Similar figures were obtained with PrP106–126 V and PrP106–126 VNH_2, sug-

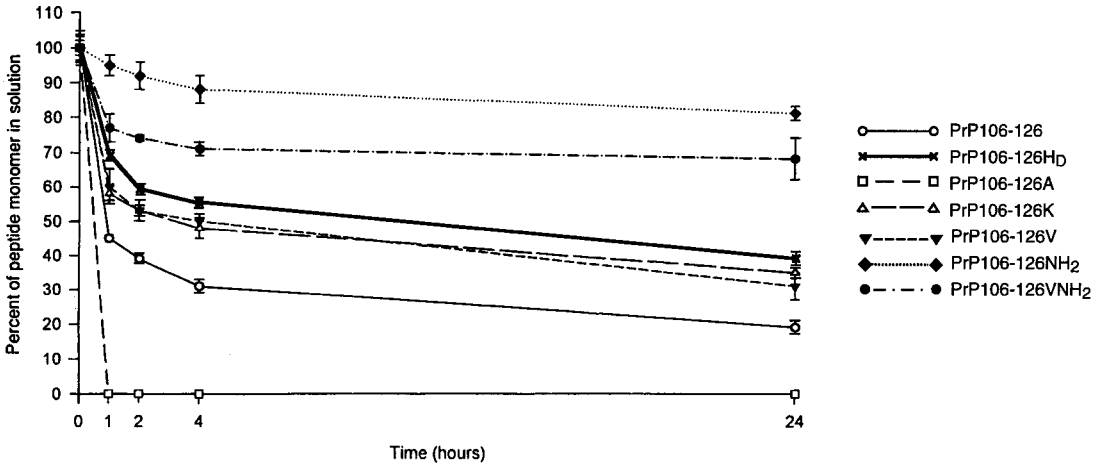

Figure 2 Sedimentation pattern of PrP106–126 and its analogues

Each point represents the percentage of peptide monomer in the 13 000 ***g*** supernatant fraction of peptide solutions in 200 mM phosphate buffer, pH 5.0, incubated at room temperature for different durations. Results are means ± S.E.M. for three determinations.

gesting that the neutral pH and the amino acid change linked to GSS disease enhance these peptides' ability to aggregate. In contrast, the increases in turbidity of the analogues carrying the substitution of D-His, Ala or Lys for L-His[111] or the amidation of Gly[126] were similar at pH 5.0 and 7.0; however, the magnitude of the increase differed between these peptides, being highest in PrP106–126 A and lowest in PrP106–126 NH_2. With regard to PrP106–126 A, the increase in turbidity occurred very rapidly and reached a plateau within 1 h (results not shown), suggesting that this peptide is highly insoluble in buffered solutions. It is noteworthy that the decrease in aggregation capacity and the sensitivity to pH variations of PrP106–126 NH_2 were partly restored by the substitution of Val for Ala[117].

These results were consistent with those obtained by HPLC determination of the proportion of the peptides that was not precipitated by centrifugation. Whereas turbidimetry revealed the aggregated fraction, sedimentation enabled us to quantify the soluble fraction. This was lowest for PrP106–126 A, followed by PrP106–126, PrP106–126 V, PrP106–126 K, PrP106–126 H_D, PrP106–126 VNH_2 and PrP106–126 NH_2. All peptides showed a decrease in soluble fraction with time; the decrease was extremely rapid for PrP106–126 A, which was already undetectable in the supernatant after 1 h owing to its high insolubility (Figure 2).

Ultrastructural and staining properties of PrP peptide assemblies

The nature of the aggregates generated by PrP106–126 and its analogues was determined by electron microscopy after negative staining and by fluorescence microscopy after treatment with thioflavin S. As reported previously, PrP106–126 formed dense meshes of straight, unbranched fibrils 4–8 nm in diameter and up to 2.0 μm long (Figure 3A). The fibrillar assemblies showed yellow fluorescence after staining with thioflavin S. Similar findings were observed with peptides with the substitution of Lys for His[111] (results not shown) and of Val for Ala[117] (Figure 3D). Conversely, PrP106–126 H_D showed a striking decrease in density, length and diameter of the fibrils (Figure 3B).

The most remarkable change in the fibrillogenic properties of the peptide was seen with PrP106–126 A, of which the aggregates consisted primarily of amorphous material and, to a smaller

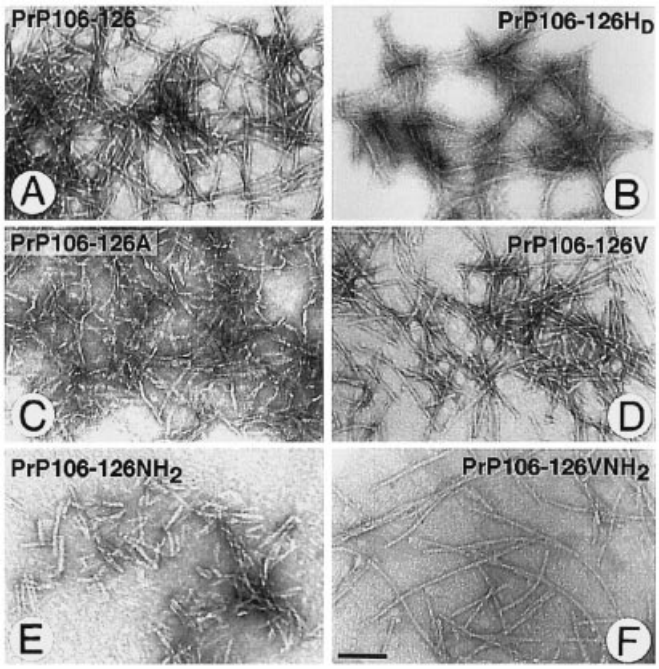

Figure 3 Electron micrographs of fibrils generated *in vitro* by PrP106–126 and its analogues

Shown are PrP106–126 (**A**), PrP106–126 H_D (**B**), PrP106–126 A (**C**), PrP106–126 V (**D**), PrP106–126 NH_2 (**E**) and PrP106–126 VNH_2 (**F**). Scale bar, 100 nm.

extent, of thin, short filamentous structures with an irregular profile (Figure 3C), lacking the staining properties of amyloid. PrP106–126 NH_2 also had a lower fibrillogenic ability than PrP106–126; this was partly restored in PrP106–126 VNH_2, whereas PrP106–126 NH_2 generated a few straight fibrils 4–8 nm in diameter and less than 0.2 μm in length (Figure 3E). The morphology and staining properties of the peptide assemblies formed by PrP106–126 VNH_2 were similar to those of PrP106–

Table 3 Effects of PrP106-126 analogues on nerve and astroglial cells

Cultures of neurons and astrocytes were exposed for 7 days to the peptides [5,6]. Neuronal viability and astroglial proliferation were estimated by a colorimetric method. Results are expressed as percentage of control and are means ± S.E.M. for six to twelve determinations. *$P < 0.01$ compared with the relevant control group (Dunnett's test).

	Nerve cell viability		Astroglial proliferation	
Peptide	Control	Peptide	Control	Peptide
PrP106–126	100 ± 5.7	23.6 ± 5.8*	100 ± 3.0	265 ± 10*
PrP106–126 NH_2	100 ± 6.2	23.0 ± 7.9*	100 ± 6.0	119 ± 4.0
PrP106–126 VNH_2	100 ± 4.8	39.9 ± 9.1*	100 ± 10	164 ± 2.0*

126 (Figure 3F); however, the fibril density was significantly lower than for the native sequence.

Biological activities of PrP106–126 analogues with different aggregation properties

Previous studies showed that the highly fibrillogenic PrP106–126 is neurotoxic and induces astroglial proliferation *in vitro*. To investigate whether these biological properties are related to the aggregation state of the peptide, primary cultures of neurons and astrocytes were exposed to analogues with diverse abilities to assemble into amyloid-like fibrils. In particular, PrP106–126 was compared with the poorly fibrillogenic PrP106–126 NH_2 and with PrP106–126 VNH_2, which had an intermediate propensity to aggregate. The study showed that the neurotoxicity of PrP106–126 analogues was not dependent on their fibrillogenic properties because all peptides induced a similar decrease in nerve cell viability after 7 days of treatment at 50 μM. Conversely, the effects on astrocytes seemed to be related to the aggregation state because PrP106–126 NH_2 was unable to induce astroglial proliferation, whereas PrP106–126 VNH_2 showed partial activity (Table 3).

DISCUSSION

The sequence comprising residues 106–126 of human PrP corresponds to a highly conserved region of the molecule, located in the flexibly disordered N-terminal segment adjacent to the structurally well-defined globular domain [9,10]. This region is required for the conversion of PrP^c into PrP^{res} [20]. Studies *in vitro* suggest that it might have a central role in the conformational change of PrP and in the pathogenesis of tissue changes associated with the accumulation of PrP^{res} in the brain [5–7,12–17].

A recent study [25] on recombinant PrP corresponding to human residues 91–231 showed that reduction of the disulphide bond between Cys^{179} and Cys^{214} resulted in a conformational change from a predominantly α-helical to a β-sheet structure. Most of this rearrangement seemed to occur within the C-terminal domain, whereas residues 91–126 were found to be unstructured in both the α-helical and β-sheet forms of the protein. The discrepancy between this observation and our results could be due to profound differences in structure and behaviour when the PrP region comprising residues 106–126 is isolated as a peptide or is a part of the PrP polypeptide chain. However, previous studies showed that the disulphide bond is required for PrP^{res} formation [20]; thus the change from α-helical to β-sheet structure after reduction of the protein might be different from that occurring *in vivo*. In this regard, it is noteworthy that the protease-resistant core of PrP^{res} corresponds approximately to residues 90–231 and includes the segment 90–125. Because this segment is flexible and protease-sensitive in PrP^c, it must undergo a significant conformational change in the conversion to PrP^{res} that precludes its accessibility to proteases.

We have previously shown that the synthetic peptide PrP106–126 adopts different conformations in different environments, although it has a high propensity to form stable β-sheet structures and to assemble into amyloid fibrils [13–15]. Because the secondary structure of the peptide is markedly influenced by pH, its physicochemical properties might be at least partly related to His^{111}, which is the only residue that changes in ionization state between pH 5.0 and 7.0 and is located in a critical region between the N-terminal polar head (KTNMKH) and the long hydrophobic tail (MAGAAAAGAVVGGLG). The relevance of His^{111} to the conformational change of PrP and the pathogenesis of prion diseases is suggested by the observations that (1) human PrP^c undergoes proteolytic cleavage between Lys^{110} and His^{111}, whereas the abnormal PrP species associated with prion diseases do not [26], and (2) transgenic mice expressing Syrian hamster PrP carrying the double substitution of the more hydrophobic residue Ile for Lys^{110} and His^{111} spontaneously develop spongiform changes and astrogliosis of the grey matter, similar to those observed in scrapie-infected mice [27].

The present study further supports the view that His^{111} is a critical site of the protein. The substitution of D-His^{111} for L-His^{111} abolished the pH-dependent conformational polymorphism of PrP106–126, caused a loss of stability of the β-sheet structure and decreased the peptide's fibrillogenic ability. Conceivably these effects are related to the fact that the orientation of the imidazole moiety of D-His is opposite to that of L-His; this might cause steric hindrance with neighbouring Lys^{110} and Met^{112} residues, inducing the formation of a random coil structure. In contrast, the substitution of the highly hydrophobic, non-ionizable residue Ala for His^{111} caused the peptide to become insoluble in buffered solutions. Although PrP106–126 A showed a high proportion of β-sheet secondary structure, it formed mainly amorphous aggregates. This is most probably due to the prevalence of the intramolecular hydrophobic forces of the lipophilic residues on the kinetics of fibril assembly. Unexpectedly, replacing His^{111} with Lys (a polar residue that is always ionized in the pH range 5.0–7.0) modified the pH-dependent structural polymorphism of the peptide, although it did not affect its ability to form amyloid fibrils. As mentioned above, His^{111} is located between the hydrophobic and hydrophilic portions of PrP106–126; this molecular environment might affect the pK_a of Lys at this site. Furthermore, the β-sheet secondary structure of PrP106–126 K was largely maintained in TFE, suggesting that its stability depends on an ionized residue at position 111.

Our results support previous observations that the β-sheet content is a key factor for amyloid fibril formation. The only exception was the substitution of Ala for His^{111}, as discussed above. Conversely, there was no simple and direct relation between the amount of β-sheet secondary structure of PrP106–126 analogues and their aggregation properties, as deduced by CD spectroscopy and turbidimetry respectively. The aggregation abilities of PrP106–126 and PrP106–126 V were greater at pH 7.0 than pH 5.0, despite both peptides' having a higher content of β-sheet structure at acidic pH. Furthermore, the quantity of aggregates of PrP106–126 K was similar at pH 5.0 and 7.0, although the β-sheet content was distinctly larger at pH 5.0. These apparent inconsistencies are due to the fact that CD spectroscopy and turbidimetry explore peptide populations in

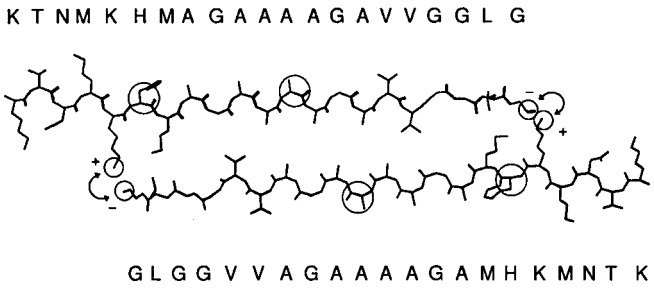

Figure 4 Proposed model of β-sheet formation by PrP106–126, showing an antiparallel alignment of two molecules of PrP106–126

The two ends of the secondary β-sheet structure are stabilized by ion-pair interactions. The residues His^{111}, Val^{117}, the N-terminal Lys^{106} and C-terminal Gly^{126} are highlighted.

different physical states (the former detects the soluble fraction, whereas the latter reveals insoluble macroaggregates), so a correlation between the two might not always be apparent. PrP106–126 and PrP106–126 V are more soluble at pH 5.0 than at pH 7.0 owing to the protonation of His^{111}, which decreases the propensity of the peptides to aggregate by antagonizing the intramolecular hydrophobic forces of the lipophilic core. This allows the presence of a larger population of monomers or oligomers in solution that are capable of adopting a β-sheet secondary structure. With PrP106–126 K, His^{111} was replaced by a residue that is not sensitive to pH change; aggregation was therefore not affected.

The contribution of the C-terminal carboxy group to the physicochemical properties of amyloid peptides has been investigated by Terzi et al. [28,29], by using the fragment 25–35 of the β-protein involved in the pathogenesis of Alzheimer disease. Removal of the C-terminal electric charge by amidation led to a predominantly random-coil structure and inhibited fibril formation. On the basis of this observation, we amidated the C-terminal Gly^{126} of PrP106–126, seeking to decrease the fibrillogenic ability of the peptide. This in turn allowed us to assess the relationship between aggregation state and biological activity as well as the influence of the substitution Val for Ala^{117} on the physicochemical characteristics. The amidation of the C-terminus abolished the molecular polymorphism of PrP106–126 yielding a predominantly random coil structure at both neutral and acidic pH, and increased the sensitivity to the helix-promoting solvent TFE. Interestingly, although this change also decreased the propensity of the peptide to generate amyloid fibrils, the fibrillogenic ability was not completely abolished. A possible interpretation of these results is that PrP106–126 molecules assemble in an anti-parallel β-pleated sheet structure, which is stabilized by head-to-tail ion-pair interactions between Lys^{106} and Lys^{110} and the carboxy group of Gly^{126} (Figure 4). Elimination of the charge at the C-terminus shifts the equilibrium towards the random-coil monomeric state. However, the finding that PrP106–126 NH_2 still forms a limited number of fibrils suggests that van der Waals interactions involving the hydrophobic segment of the peptide contribute to fibril assembly.

Among prion-related encephalopathies, GSS disease is characterized by the highest degree of parenchymal amyloid [30]. This disorder segregates with mutations of the PrP gene. Because one of these mutations (i.e. $Ala^{117} \rightarrow Val$) is contained in the PrP106–126 region, we studied its effects on the peptide's conformational and fibrillogenic properties. Valine is a well-known β-sheet structure promoter [31,32] that increases the hydrophobic profile of the C-terminal part of PrP106–126. By molecular dynamic simulations of a similar peptide, PrP109–122, Kazmirski et al. [33] found that substitution of Val for Ala^{117} was the only helix-destabilizing modification of a variety of replacements with hydrophobic amino acid residues [33]. PrP106–126 V did not demonstrate a fibrillogenic ability superior to that of PrP106–126. However, the importance of this substitution was apparent by comparing PrP106–126 NH_2 and PrP106–126 VNH_2, because neither had a carboxy contribution to aggregation. The presence of Val at position 117 increased the aggregation properties of the amidated peptide; fibril morphology was very similar to that of PrP106–126.

With regard to the relationship between aggregation state and biological activity of PrP peptides, our results indicate that amyloid fibrils are not required for neurotoxicity because the effects of PrP106–126 NH_2 on primary neuronal cultures were similar to those of the wild-type sequence. Conversely, under our experimental conditions, astroglial proliferation seemed to be related to the presence of amyloid fibrils. Therefore it is possible that astrogliosis in prion encephalopathies without amyloid deposits is a mediated effect (e.g. microglia-dependent) rather than a direct effect of disease-specific PrP isoforms.

In conclusion, our results support the view that the PrP region spanning residues 106–126 is susceptible to conformational transition and might be the nido at which the conversion of PrP^{c} to PrP^{res} is initiated. Furthermore, evidence suggests that, within this region, His^{111} is important to the structural flexibility as well as the stability of the newly formed β-sheet structure. PrP106–126 and PrP106–126 NH_2 can be considered to be complementary models for investigation of the pathogenesis of prion diseases. The former is suitable for short-term studies *in vitro*; however, its use is limited by its poor manageability. This is at least partly related to the free carboxy ion on Gly^{126}, which is moreover not present in the intact protein. Removal of this charge results in a peptide that retains neurotoxic activity and mimics the slow kinetics of fibril formation observed *in vivo* in prion-related encephalopathies.

This work was supported by the Italian Ministry of Health, Department of Social Services, Telethon-Italy (grants E.254, E.449 and E.574), and the European Community (BMH4 CT96-0601, CT98-6011 and CT98-6051).

REFERENCES

1 Prusiner, S. B. (1991) Science **252**, 1515–1522
2 Bolton, D. C., McKinley, M. P. and Prusiner, S. B. (1982) Science **218**, 1309–1311
3 McKinley, M. P., Bolton, D. C. and Prusiner, S. B. (1983) Cell **35**, 57–62
4 DeArmond, S. J., McKinley, M. P., Barry, R. A., Braunfeld, M. B., McColloch, J. R. and Prusiner, S. B. (1985) Cell **41**, 221–235
5 Forloni, G., Angeretti, N., Chiesa, R., Monzani, E., Salmona, M., Bugiani, O. and Tagliavini, F. (1993) Nature (London) **362**, 543–546
6 Forloni, G., Del Bo, R., Angeretti, N., Chiesa, R., Smiroldo, S., Doni, R., Ghibaudi, E., Salmona, M., Porro, M., Verga, L. et al. (1994) Eur. J. Neurosci. **6**, 1415–1422
7 Brown, D. R., Schmidt, B. and Kretzschmar, H. A. (1996) Nature (London) **380**, 345–347
8 Riek, R., Hornemann, S., Wider, G., Billeter, M., Glockshuber, R. and Wüthrich, K. (1996) Nature (London) **382**, 180–182
9 Riek, R., Hornemann, S., Wider, G., Glockshuber, R. and Wüthrich, K. (1997) FEBS Lett. **413**, 282–288
10 Donne, D. G., Viles, J. H., Groth, D., Mehlhorn, I., James, T. L., Cohen, F. E., Prusiner, S. B., Wright, P. E. and Dyson, H. J. (1997) Proc. Natl. Acad. Sci. U.S.A. **94**, 13452–13457
11 Caughey, B. W., Dong, A., Bhat, K. S., Ernst, D., Hayes, S. F. and Caughey, W. S. (1991) Biochemistry **30**, 7672–7680
12 Pan, K. M., Baldwin, M., Nguyen, J., Gasset, M., Serban, A., Groth, D., Mehlhorn, I., Huang, Z., Fletterick, R. J., Cohen, F. E. and Prusiner, S. B. (1993) Proc. Natl. Acad. Sci. U.S.A. **90**, 10962–10966
13 Tagliavini, F., Prelli, F., Verga, L., Giaccone, G., Sarma, R., Gorevic, P., Ghetti, B., Passerini, F., Ghiabaudi, E., Forloni, G. et al. (1993) Proc. Natl. Acad. Sci. U.S.A. **90**, 9678–9682

14 Selvaggini, C., De Gioia, L., Cantù, L., Ghibaudi, E., Diomede, L., Passerini, F., Forloni, G., Bugiani, O., Tagliavini, F. and Salmona, M. (1993) Biochem. Biophys. Res. Commun. **194**, 1380–1386
15 De Gioia, L., Selvaggini, C., Ghibaudi, E., Diomede, L., Bugiani, O., Forloni, G., Tagliavini, F. and Salmona, M. (1994) J. Biol. Chem. **269**, 7859–7862
16 Brown, R. D., Herms, J. and Kretzschmar, H. A. (1994) Neuroreport **5**, 2057–2060
17 Brandner, S., Isenmann, S., Raeber, A., Fischer, M., Sailer, A., Kobayashi, Y., Marino, S., Weissmann, C. and Aguzzi, A. (1996) Nature (London) **379**, 339–343
18 Diomede, L., Sozzani, S., Luini, W., Algeri, M., De Gioia, L., Chiesa, R., Lievens, P. M., Bugiani, O., Forloni, G., Tagliavini, F. and Salmona, M. (1996) Biochem. J. **320**, 563–570
19 Salmona, M., Forloni, G., Diomede, L., Algeri, M., De Gioia, L., Angeretti, N., Giaccone, G., Tagliavini, F. and Bugiani, O. (1997) Neurobiol. Dis. **4**, 47–57
20 Muramoto, T., Scott, M., Cohen, F. E. and Prusiner, S. B. (1996) Proc. Natl. Acad. Sci. U.S.A. **93**, 15457–15462
21 Yang, J. T., Wu, C. S. and Martinez, H. M. (1986) Methods Enzymol. **130**, 208–269
22 Andreoni, G., Angeretti, N., Lucca, E. and Forloni, G. (1997) Exp. Neurol. **148**, 281–287
23 Yao, J., Keri, J. E., Taffs, R. E. and Colton, C. A. (1992) Brain Res. **591**, 88–93
24 Chiesa, R., Angeretti, N., Lucca, E., Salmona, M., Tagliavini, F., Bugiani, O. and Forloni, G. (1996) Eur. J. Neurosci. **8**, 589–597
25 Jackson, G. S., Hosszu, L. L. P., Power, A., Hill, A. F., Kenney, J., Saibil, H., Craven, C. J., Waltho, J. P., Clarke, A. R. and Collinge, J. (1999) Science **283**, 1935–1937
26 Chen, S. G., Teplow, D. B., Parchi, P., Teller, J. K., Gambetti, P. and Autilio-Gambetti, L. (1995) J. Biol. Chem. **270**, 19173–19180
27 Hegde, R. S., Mastrianni, J. A., Scott, M. R., DeFea, K. A., Tremblay, P., Torchia, M., DeArmond, S. J., Prusiner, S. B. and Lingappa, V. R. (1998) Science **279**, 827–834
28 Terzi, E., Holzemann, G. and Seelig, J. (1994) Biochemistry **33**, 1345–1350
29 Terzi, E., Holzemann, G. and Seelig, J. (1994) Biochemistry **33**, 7434–7441
30 Ghetti, B., Piccardo, P., Frangione, B., Bugiani, O., Giaccone, G., Young, K., Prelli, F., Forlow, M. R., Dlouhy, S. R. and Tagliavini, F. (1996) Brain Pathol. **6**, 127–145
31 Branden, C. and Tooze, J. (1991) in Introduction to Protein Structure (Branden, C. and Tooze, J., eds.), pp. 247–267, Garland Publishing, New York
32 Warwicker, J. and Gane, P. J. (1996) Biochem. Biophys. Res. Commun. **226**, 777–782
33 Kazmirski, S. L., Alonso, D. O., Cohen, F. E., Prusiner, S. B. and Daggett, V. (1995) Chem. Biol. **2**, 305–315

Received 22 March 1999/13 May 1999; accepted 10 June 1999